SoftER: A Spiral Soft Robotic Ejector for Sorting Applications

Ilias Zournatzis, *Graduate Student Member, IEEE*, Sotiris Kalaitzakis, and Panagiotis Polygerinos, *Senior Member, IEEE*

***Abstract*—For over thirty years optical belt drive configurations are being used in food industries to automatically sort produce in high operating speeds. Despite their benefits, these multi-component assemblies are prone to faults, difficult to clean, and require frequent maintenance that halts the production lines for considerable amount of time. In this letter, we adopt the abundantly occurring spiral motions encountered in nature and translate them to the proof-of-concept design and development of a soft pneumatic actuator (SPA), the SoftER. This novel actuator has the ability to rapidly unwind when pressurized to deliver impact forces. We explore this inherently low-cost and simple design and its potential to replace current systems based on the results of an application case study presented in this letter. Simulation driven optimization methods are leveraged, utilizing quasi-static and dynamic finite element methods models, to create a scalable framework for selecting the best performing design parameters for each application. Using rapid manufacturing processes the optimized actuator is constructed and physical testing validates its high-speed and impact force delivering capabilities.**

***Index Terms*—Soft sensors and actuators, soft robot applications, soft robot materials and design.**

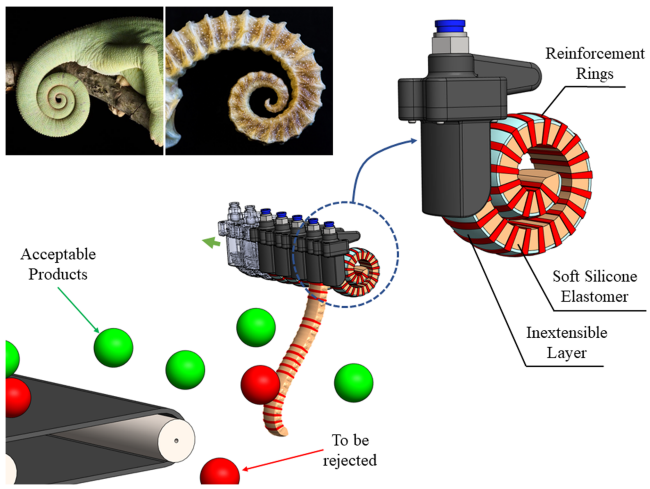

Fig. 1. Proposed bio-inspired design for sorting applications that utilizes the SoftER spiral soft pneumatic actuator.

I. Introduction

THE Automated Sorting Machines (ASM) global market, in 2021 was valued at approximately 4.1 billion USD and is expected to grow to 6.1 billion USD until 2028 at a Compound Annual Growth Rate (CAGR) of 5.9% [1]. An ASM pertains to a complex system being able to receive feedback from what is usually a high-volume production line, and actuate certain mechanical components to reject faulty products. Indications on the sorting criteria could be weight, size, shape, or color among others. The primary reasons for using ASMs in production environments, are twofold; (i) to minimize faulty products in a production batch via an automatised manner, and (ii) to maximize production yield by neglecting the bottleneck introduced by a human worker.

One of the most commonly used industrial sorting solutions involves an optical conveyor belt system for rejecting faulty products [2]. These systems are installed in-line with the product infeed, and use an optical feedback system to track faulty products in real-time, based on criteria such as color, shape, or size. After identifying the defective products, a pneumatically actuated system is able to reject them, based on high-speed trajectory calculations (Fig. 2). Examples of sorting processes abound in the food industry, where food safety certifications and high production volumes make effective sorting critical, such as the ability to separate ripe from unripe fruit [3], [4], [5], [6].

There are usually two approaches for rejecting defective products. Lighter systems that handle smaller and lighter products (e.g. nuts, pills, packages, etc.) use an array of nozzles and leverage the power of high-speed air jets to isolate a product from the rest of the production. For bigger, and thus heavier products (e.g. apples, potatoes, tomatoes, etc.) an array of paddles actuated by pneumatic cylinders is used, that rejects products using a rapid swinging motion. When a faulty product is identified, the corresponding cylinder in line with that item is rapidly

Manuscript received 9 May 2023; accepted 1 September 2023. Date of publication 13 September 2023; date of current version 21 September 2023. This letter was recommended for publication by Associate Editor T. Nanayakkara and Editor C. Laschi upon evaluation of the reviewers' comments. The work of Ilias Zournatzis was supported by Bendabl SMPC, Athens, Greece (bendabl.com). This work was supported in part by Bendabl SMPC, Athens, Greece (bendabl.com), in part by the European Union through the PALPABLE Project for the study of design methodologies and optimisation principles for radially constrained SPAs under Grant 101092518, and in part by HEAL-Link for the publication of the article in OA mode. *(Corresponding author: Panagiotis Polygerinos.)*

Ilias Zournatzis is with the Control Systems and Robotics Laboratory School of Engineering, Hellenic Mediterranean University, 71004 Heraklion, Greece, and also with Bendabl SMPC, 11855 Athens, Greece (e-mail: ddk158@edu.hmu.gr).

Sotiris Kalaitzakis and Panagiotis Polygerinos are with the Control Systems and Robotics Laboratory School of Engineering, Hellenic Mediterranean University, 71004 Heraklion, Greece (e-mail: tm6613@edu.hmu.gr; polygerinos@hmu.gr).

This letter has supplementary downloadable material available at https://doi.org/10.1109/LRA.2023.3315206, provided by the authors.

Digital Object Identifier 10.1109/LRA.2023.3315206

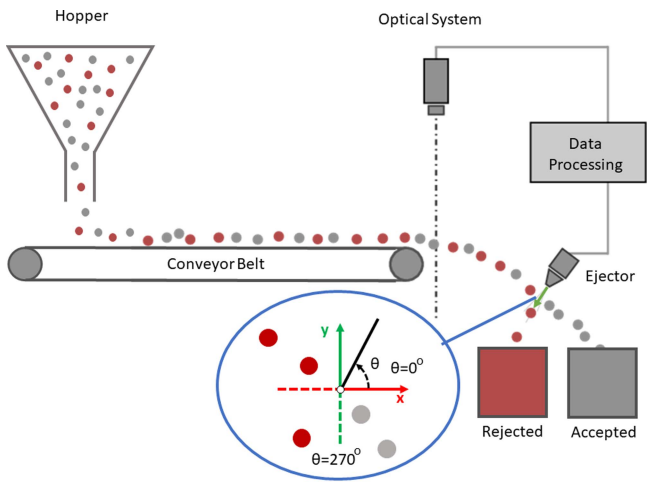

Fig. 2. Standard optical belt drive sorting system comprising of a hopper, conveyor belt, optical feedback system, and pneumatic ejector.

compressed with air, subsequently pushing a paddle forward to intersect it at its trajectory and separate it from all others. Although this method is used from the 1980's [7], designing and maintaining these machines is still significantly complex due to the multi-component assemblies, number of fasteners, and laborious disassembling. ASMs should be built as simple as possible and thus maintenance, repair, and adjustment should be a task to perform with minimal time and expense [2].

This work proposes an alternative that aims to improve performance, minimize downtime and cost per unit, and optimize assembly complexity by leveraging the flexibility put forth by the field of soft robotics. We propose SoftER (i.e., Soft sortER), a bio-inspired modular soft pneumatic actuator for sorting applications (Fig. 1). Over the past decade, soft actuator designs have been proposed that focus mostly on actuation speed and adaptability, rather than force output [8]. Other types of actuators have been developed that focus in instantaneous force output [9] but to our knowledge not considerable work has been done towards targeting both speed and force output in a single unit. Only recently new types of preshaped curved actuators have emerged [10], [11], that utilise inherently flexible materials and pneumatic actuation to deliver rapid movements with high power density and minimal assemblies [12], [13], [14], [15], [16]. This work proposes a soft pneumatic actuator that attempts to target both high speed applications with a concentrated force density. Additionally, in this work, we describe a novel methodology on simulating highly dynamic movement using FEA Explicit Dynamic simulations. To our knowledge, this hasn't been explored sufficiently in the current SOA. To that end we believe that our work puts forth methodologies for predicting the qualitative performance of rapidly actuated SPAs in highly dynamic environments. We believe that this can significantly help with the design of such actuators through simulated driven design.

The proposed design, when in free state, is wrapped in a preshaped spiral configuration. When a pressurised gas (e.g. air) is inserted into the system the actuator expands rapidly, performing an unwinding motion, thus intersecting the desired object from its original trajectory.

In this letter we analyze the design and development process of SoftER. More specifically, in Chapter II the design requirements are discussed following an industry-focused approach. The design methodology and fabrication approaches are presented by leveraging CAD parametric design and rapid prototyping processes. In Chapter III we present the simulation-driven optimisation of the proposed actuator using Finite Element Analysis. Finally, in Chapter IV the experimental characterization of an actuator module is described.

II. Soft Sorter Development

A. Soft Sorter Requirements

The system performance requirements for a soft robotic ejector for sorting applications vary greatly and are dependent on the specific application (i.e. industrial requirements, operational conditions, product size, weight, shape, etc.). On this section we provide general guidelines on designing a soft robotic ejector. One can easily tailor application-specific requirements from a combination of review of the literature, practical considerations, theoretical studies, and observation of publicly available industrial examples. One of the first high-level considerations is the operating range of air-pressure of the soft actuator. A high-flow, high-pressure pneumatic line is preinstalled in the majority of industrial settings that perform sorting operations.

A main consideration is the rejection speed of the goods as well as the required force to reject them as these follow a high-speed trajectory out of a conveyor belt. Indicatively, a peach can weigh from 15 to 150 grams and have an average diameter ranging from 2–8 cm. Beside the weight of an object, impact forces can vary greatly as they are also dependent of the object velocity at the time of impact. It is noted that the lower forces generated by an ejector are still adequate to alter the initial travel trajectory upon impact. As sorting machines come with conveyor belts, the width of each ejector module is required to be a small fraction of it.

Final considerations for the SoftER actuator include its ability to operate with minimal intervention and maintenance. One of the major issues with existing sorting machines is the down-time for maintenance and replacement of a cylinder-paddle ejector. Due to the multi-component assembly that comprises them, any time halts of the sorting process are considerable. In this work the ejector replacement requirement is set to a much lower time value of about one minute, to account the need for shorter duration down-times.

B. Soft Sorter Design

Mathematical patterns such as spirals can often be observed in nature. Weather phenomena, animals, plants and other formations can often exhibit patterns that resemble or clearly follow a spiral (Fig. 1-inset) [17]. Classical mechanisms and continuum structures that leverage spiral mechanisms have been designed that take advantage of the energy storage potential of an unwinding motion to exert high forces, manipulate objests, or transverse terrains [10], [18], [19], [20], [21]. However, most of the robots presented by the current literature focus on manipulation or

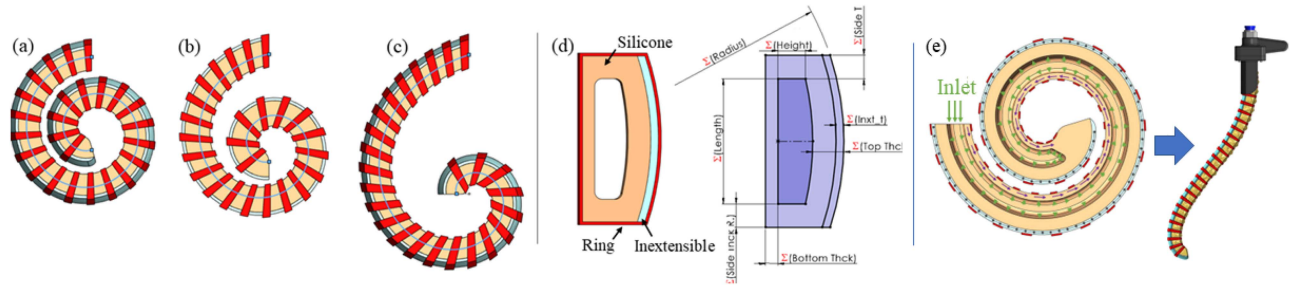

Fig. 3. SPAs with: (a) Archimedes's spiral as a centerline. (b) Natural logarithmic spiral. (c) Logarithmic spiral variation based on Golden ratio. (d) SPA cross section. (e) Pressurization body in cross section and unwinded pressurized shape.

locomotion, tasks that require slowly occurring actuation. There has not been sufficient efforts in designing and characterising robotic systems that are inspired by natural patterns and can perform highly dynamic movements, such as the ones required for rapid sorting applications. The proposed SPA follows a bio-inspired design and is comprised of three main modules, all integrated into a single spiral component (Fig. 1): (i) The soft body made of silicone elastomer with an inner hollow chamber that runs the entire length of the actuator; (ii) an inextensible layer integrated into the soft body made from woven fabric, and (iii) reinforcement rings made from hard plastic (i.e. PLA). These three modules combined are responsible for the rapid unwinding motion of the spiral SPA when pressure is applied to the inner chamber.

During free space actuation the motion is pre-programmed in two ways. (i) The reinforcement rings prevent the radial expansion directing the strain energy towards expanding the SPA along its axial direction. This constraint enables the rapid unwinding of the spiral SPA. (ii) The inextensible layer prevents axial extension of the top layer of the actuator. By introducing a component that is able to freely curl but not deform under tensile loads, energy that would otherwise be wasted in extension deformation is now channeled and fully utilized in the unwinding motion (Fig. 3(e)).

The most common spirals that can be observed in nature can be expressed through mathematical models of (a) the Archimedes's spiral, (b) the Fibonacci spiral, (c) the Golden spiral, and (d) the Logarithmic spiral [17]. Based on the Archimedes's spiral, the Logarithmic spiral, and the Golden spiral as centerline curves, three SPAs are designed based on soft robotic design principles (Fig. 3).

Initially, the three spiral actuators are tested quasi-statically using Finite Elements Methods modeling (Section III) to assess the different pressure requirements for a complete unwinding motion up to the point of impact. This is considered to be approximately at a contact angle with the object for rejection of $\theta = 270^o$ where according to simple calculations the maximum impact force for a paddle sorting actuator, that acts as a single link rotational arm, can be delivered (Fig. 2-inset). The three actuators are designed preserving the same design variables so as to equally compare their motion profiles and fully parameterize the SPA design (Fig. 3). The parameters used for all three spiral type SPAs are within the ejector characteristic design requirements (Section II-A) and are presented in Table I.

TABLE I
CONFIGURATION VARIABLES FOR DESIGN COMPARISON

Design Variable	Value	Design Variable	Value
Sweep curve	142mm	Cross Section	56mm^2
Top Thickness	4mm	α_a	2
Side Thickness	3mm	α_l	3.2
Bottom Thickness	1.6mm	b_l	0.18
No. of Rings	25	α_g	0.94

To design the centerline curves for the three novel actuators the corresponding equations in polar coordinates are used. The mathematical representation of a spiral in a polar coordinate system considers two variables, (i) the distance from the origin r, and (ii) the corresponding angle θ. Thus, the Archimedes' spiral is defined as [22]: $r = \alpha_a \cdot \theta$ where, α_a is a constant coefficient. The logarithmic spiral is similarly defined [23] based on: $r = \alpha_l \cdot e^{b_l \cdot \theta}$ where, α_l and b_l are arbitrary constant coefficients.

Finally, a variation of the logarithmic spiral is defined as the Golden Spiral. This mathematical curve is based on Archimedes' but instead of using Euler's number as base, the Golden Ratio ϕ, defined as $\phi = 1.618$, is used [23]. The resulting equation is defined for a growth factor of $b = 2/\pi$ as: $r = \alpha_g \cdot \phi^{2/\pi \cdot \theta}$ where, α_g is a constant coefficient.

C. Soft Sorter Manufacturing

The fabrication of the proposed actuators is based on two rapid prototyping techniques using Fused Filament Fabrication (FFF) 3D printing and two-part silicone casting. The necessary files are generated directly from the CAD model of the actuator and the following steps are completed as presented in Fig. 4. Using the soft silicone part of the SPA, a mold is designed through Boolean subtraction from a block geometry. The mold is split in two parts to enable easy de-molding and exhaust holes, as well as a silicone pouring hole, are incorporated in the design. The final mold is 3D printed using PLA plastic.

Similarly, a soft core geometry is designed to enable the formation of the inner chamber that will be pressurized during actuation. The soft core is printed using flexible TPU filament to enable its removal after the de-molding process.

During silicone casting, a two-parts silicone with shore hardness 20 A (Dragon Skin 20, Smooth-On) is mixed in a 1:1 ratio along with a few drops of coloring pigment. The mixed silicone compound is then placed in a vacuum chamber to extract trapped air bubbles that could become stress concentration spots

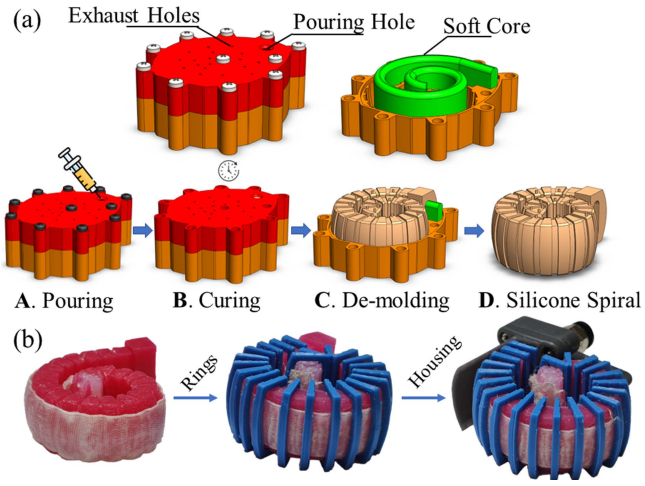

Fig. 4. (a) Silicone molding process. (b) Assembly of the SoftER SPA module.

during actuation. The selection of DragonSkin 20 constitutes a mid-range solution in the field of soft robotics materials. For this work, we focused the analysis of the actuator on the geometric design and selected a material based on previously studied properties [24], as well as a technical expertise acquired by our team in previous research [8], [25].

Following the steps presented in Fig. 4, the silicone is poured to the sealed mold using a syringe until the complete volume has been filled. Subsequently, the mold is placed in an oven (Form Cure, FormLabs) at a temperature of 50 ^{o}C for 30 minutes. The cured silicone is removed from the mold and the soft core is elicited manually to free up the inner cavity of the actuator. A strip of woven fabric is adhered (Sil-Poxy, Smooth-On) on the outer layer of the SPA and any defects are sealed. Rigid rings are 3D printed using PLA plastic and installed manually on the dedicated grooves located on the surface of the SPA. Finally, the SPA module is coupled to a dedicated fixture equipped with a pneumatic push-in fitting for easy pressurization.

III. Finite Elements Method Modelling

A. Hyperelastic Material Modelling

To characterize the hyperelastic behavior involved in the proposed application, incompressible materials are assumed and a 2nd order Yeoh model is employed expressed as $W = C_{10}(\bar{I}_1 - 3) + C_{20}(\bar{I}_1 - 3)^2$.

Both the silicone body and inextensible layer of the SPA can be expressed through the Yeoh model while the PLA rings are modelled with a virtually infinite stiffness to obtain the rigid performance required by the reinforcements. The coefficients used for the characterization of the materials are drawn from the literature for the hyperelastic components [24] and are manually inserted for the elastic ones according to Hooke's law. These are summarized in Table II.

B. Finite Element Methods Analysis-ABAQUS CAE

Using Finite Element Methods (FEM) analysis the design of the SPA is validated and subsequently optimized through rapid design iterations. The proposed SPA is evaluated using the Abaqus 6.14 Computer Aided Engineering (CAE) package (Simulia, Dassault Systems). The FEM evaluations are performed in two stages: (i) Quasi-Static evaluation of the different spirals is performed using the Dynamic/Implicit solver. The three spirals considered (Archimedes's, Logarithmic, Golden) are evaluated under common design configurations and pressure profiles and assessed according to their unwinding potential under different pressures. (ii) Dynamic analysis of the most efficient spiral is performed using the Dynamic/Explicit solver, considering first a Design of Experiments (DOE) approach to assess the influence of different design parameters on the force output and speed of the proposed actuator. The methodology and results along with the DOE approach are presented in Section III-C. For both the Quasi-Static and Dynamic analyses similar configurations of contact definitions and meshing operations are considered for consistency. The FEM configurations that are common between the two and offer robust conditions for modelling the SoftERs are shown in Table III.

For contact definitions a Tie constraint is used to bond together the inextensible layer with the silicone body as well as the top and bottom faces of the reinforcement rings with the inextensible layer and silicone body respectively. The remainder of contact definitions are modelled using frictionless interaction properties to restrict mesh overlapping and effectively model contacts between bodies. In the Quasi-Static analysis each of the spirals is subjected to gravitational forces and a pressure input that is applied to the internal walls of the actuator cavity up to 0.24 MPa in a ramp profile.

The results demonstrate an advantage of the Logarithmic spiral regarding its unwinding potential when compared with the other two designs at similar input pressures, a result that is validated also in [10]. As shown in Fig. 5(a) and (b), the logarithmic and golden spirals are also able to achieve a complete unwinding motion exceeding the required working space of the actuator. Given the unwinding performance of the logarithmic spiral, it is selected for further investigation.

TABLE II
FEM Material Properties/Coefficients

Material	C_{10}	C_{20}	Young's Modulus-E (MPa)
Silicone	0.096	0.0095	-
Inext. Layer (hybrid)	20	0	-
Reinforcement Rings	-	-	20000

TABLE III
FEM Configuration for Spiral Design Comparison

FEA Element	Dynamic,Implicit	Dynamic,Explicit
Silicone Model	Yeoh (2^{nd} Order)	Yeoh (2^{nd} Order)
Inextensible Model	Yeoh (1^{st} Order)	Yeoh (1^{st} Order)
Reinforcement Model	Hookean	Hookean
Hyperelastic Element	C3D10H (Std,Qdrtc)	C3D10H (Exp,Qdrtc)
Elastic Element	C3D8R (Std,Lnr)	C3D8R (Exp,Lnr)
Silicone Seed	2.0	2.0
Inextensible Seed	2.5	2.5
Ring Seed	1.0	1.0

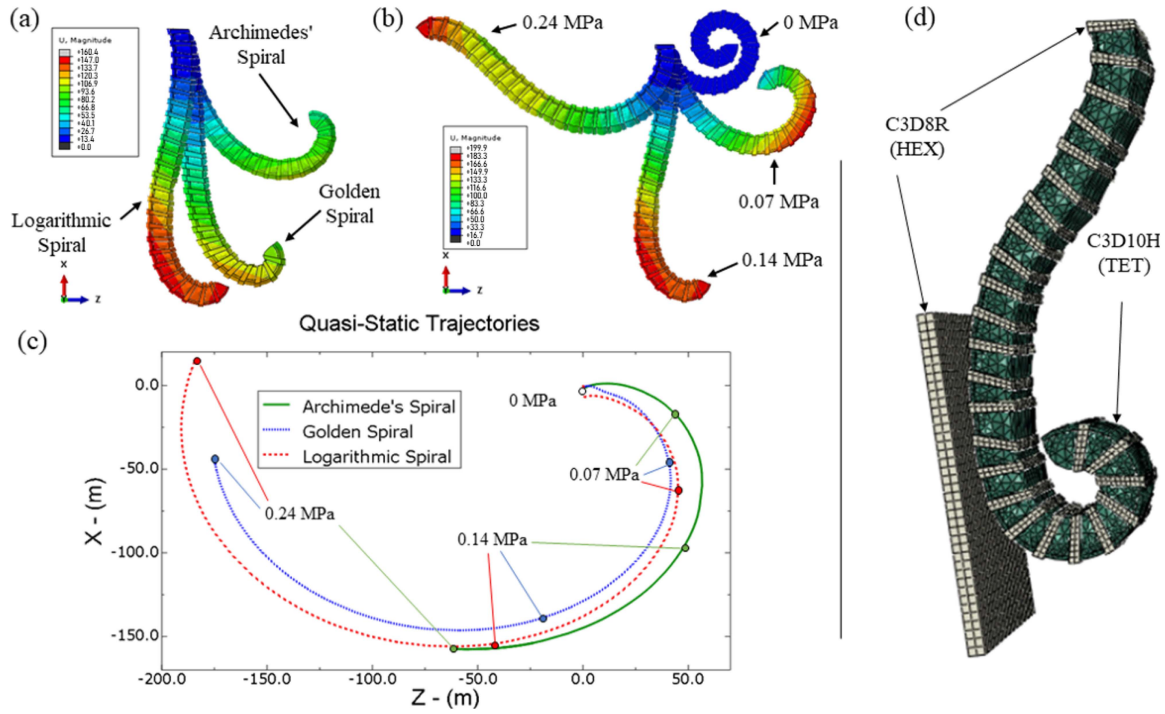

Fig. 5. (a) Different spiral unwinding formation at 0.14 MPa. (b) Full actuation cycle of logarithmic spiral. (c) Quasi-Static trajectories of different spiral endpoints. (d) Dynamic-Explicit analysis of HEX-TET combined meshes for force plate impact.

TABLE IV
DESIGN POINTS FOR RESPONSE SURFACE STUDY

Factor	Min	Max	Mean	Std. Dev.
BT-Bottom Thickness (mm)	1.50	3.00	2.25	0.5303
CS-Chamber Section (mm^2)	40.00	88.00	64.00	16.97
TT-Top Thickness (mm)	2.50	5.50	4.00	1.06

C. Design of Experiments for SoftER Optimization

A Response Surface study has been conducted (Design Expert 13, StatEase) to calculate the optimal configuration of design variables towards maximizing the applied force and actuation frequency for an exploratory number of parameters. The results of this analysis are based on a fractional factorial Box-Behnken design that considers three factors, three levels and two responses. According to the cross section of Fig. 3, bottom thickness (BT), top thickness (TT), and chamber section (CS) are selected as the primary driving parameters. Based on the nature of the problem 13 runs are considered, while including five central points for statistical stability. The design points are summarized in Table IV.

Thirteen dynamic FEM simulations are performed where each actuator is pressurized until it collided with a force plate placed in the nominal point of impact (Fig. 5(d)). During impact, the total reaction force developed on the force plate's surface is calculated. Similarly, the time for an actuation cycle (i.e. from the moment of pressurisation up to the moment of impact) is recorded. In cases where the actuator is unable to reach the force plate a force output of 0 N and an actuation frequency of 0 Hz are considered. To perform a comparative study between the various SoftER configurations the responses are normalized.

Three response models are evaluated, Linear, Quadratic, and 2FI. For all responses, the most adequate statistical stability and satisfactory coefficient of determination (R^2) is provided by the linear model. The data set is fitted to the model and the correlation matrix and response curves and combinations for each of the factors are generated (Fig. 6).

Based on the results, the most influential factor to the SoftER's speed and force capabilities is the bottom thickness with a correlation value of 0.632 and 0.569 respectively, where 1,-1 represent the complete positive/negative correlation of two statistical values. Second is the top thickness of the actuator with correlation values of -0.223 and -0.609 and finally the area of the chamber section has the least effect on performance with correlation values of 0.164 and -0.098.

To indicate the optimal configuration of design factors two linear surface models are used. Within the solution space that is defined in Table IV, the optimal parameters are calculated as: (i) BT = 3 mm, (ii) CS = 62.455 mm^2, and (iii) TT = 2.5 mm. For the two most influential factors the calculated configuration can also be derived in Fig. 6.

IV. SOFT SORTER EVALUATION

To evaluate the performance of the SoftER using the indicative configuration parameters calculated in this study an experimental platform is designed and constructed. The setup (Fig. 7) makes use of a three degrees of freedom linkage that carries a 200 N load cell and amplifier (HX711, OEM) operating at 10 HZ or 80 Hz sampling frequency with a contact plate at its distal end. At the top of the setup the SoftER is securely fixed with the spiral facing towards the ground. The position of the

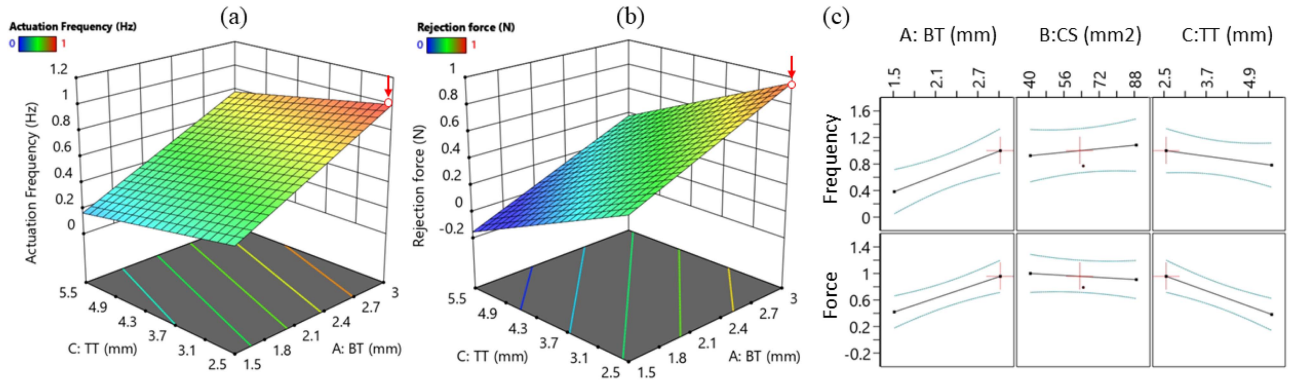

Fig. 6. Response surfaces for actuation frequency (a) and force (b) as a function of BT and TT. (c) DOE correlation curves.

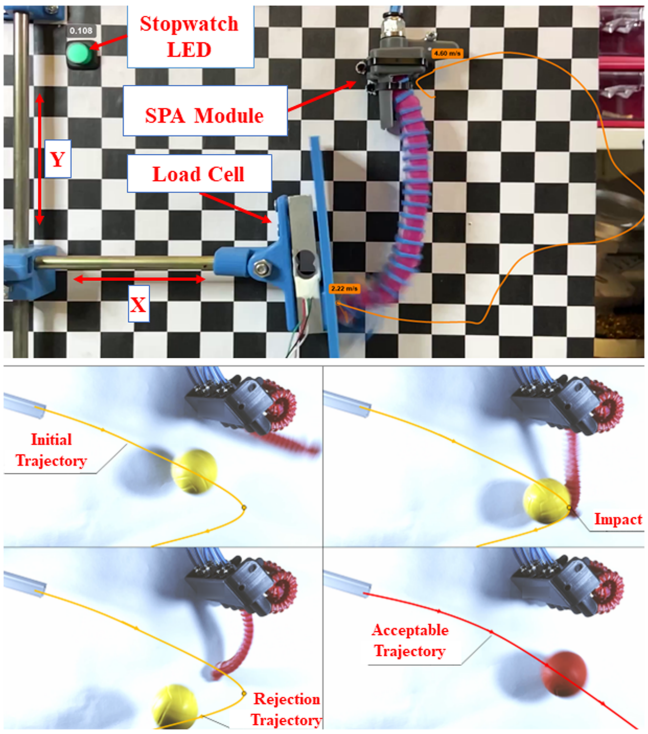

Fig. 7. Top: SoftER force and trajectory testing with experimental setup. Bottom: Sorting simulation experiment.

load cell is adjustable, in the x, y directions and theta rotation, relative to the SoftER so as to simulate a range of contact (i.e., rejection forces) scenarios at different distances and angles. A printout of a checkerboard is also placed in the background to allow for camera alignment and lens distortion corrections.

The SoftER is connected to a solenoid valve and programmed with the use of a micro-controller to pressurize for different time intervals. The spiral actuator performs a series of timed actuation cycles until contact could be established with the force plate. Fig. 7 shows the SoftER's tip trajectory where its velocity is estimated using an image processing software (Kinovea 0.9.5) as this is pneumatically pressurized from 0.28 to 0.66 MPa at 0.07 MPa increments. This indicative experiment demonstrates that rapid actuation cycles can be achieved, with the fastest measured at ≈108 ms while being able to register impact loads

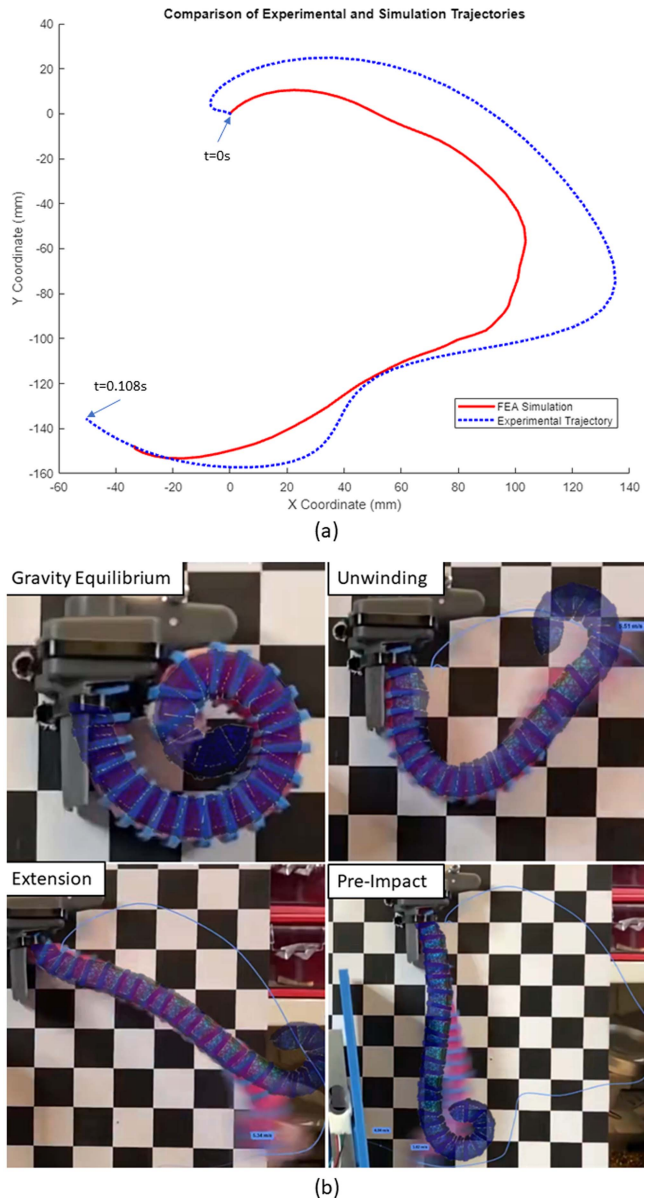

Fig. 8. Simulated vs Experimental comparisson of the actuator tip trajectory at 0.66 MPa pressurisation (a). Overlaid comparisson of actuator shape during the four phases of inflation, Gravity Equilibrium, Unwinding, Extension, and Pre-Impact (b).

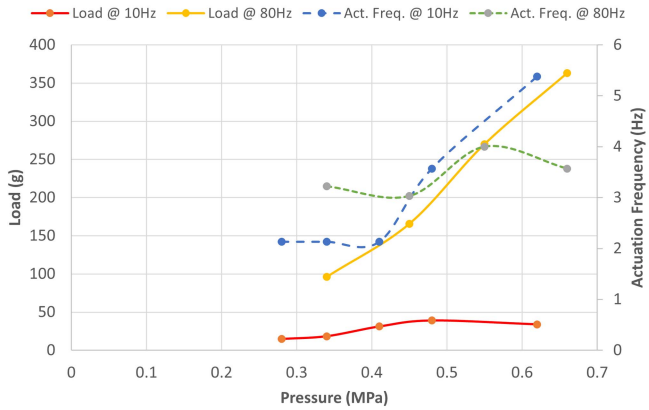

Fig. 9. SoftER load capacity and actuation frequency (3-trial mean) for pressures ranging from 0.28 to 0.66 MPa.

of up to 400 g (Fig. 9 and 7). For the fastest configuration, using the aforementioned image processing software, XY trajectory coordinates at the tip of the actuator have been extracted. Considering the corresponding simulated coordinates extracted from ABAQUS, a validation plot is presented in Fig. 8(a) along with a grid figure portraying the four phases of inflation in both experiment (opaque) and simulated actuator deformations (transparent) (Fig. 8(b)).

A Root Mean Squared Error (RMSE) value between experimental and simulated results was calculated for X and Y coordinates as RMSE = (22.8, 20.5) in (mm). The total error validates the qualitative performance of the FEA model to predict the shape morphing capacity of rapidly actuated SPAs. However, further fine-tuning is required to improve the quantitative accuracy of such models that will be carried out in future work. The experimental measurements are recorded using an 80 Hz sampling rate which provided an order of magnitude higher results than the 10 Hz registration experiments. For that reason and to test the validity of the application a sorting simulation experiment is conducted where a series of SoftER modules are used to reject objects weighing approximately 100 g–150 g and traveling at speeds of $\approx$1 m/s (Fig. 7).

V. Conclusion

In this work the proof-of-concept of a novel soft spiral actuator was presented, named SoftER, able to unwind at high speeds and deliver impact forces. To the best of our knowledge this is the first time a soft actuator was designed with the goal to identify a better alternative to existing sorting ejectors that are costly, comprise of multiple components prone to faults, and require frequent downtime for repairs. The bio-inspired SoftER underwent a thorough parametric study with both quasi-static and dynamic computational models and a parameters based framework was established for its performance. The specific values of the parameters were tuned in a fractional factorial optimization study, which was conducted to identify the best performing configuration within the example solution space. The fabrication steps were presented and a physical version of the optimum design was constructed and tested in an experimental setup. The experiments validated that the SoftER was able to reach high actuation frequencies and rejection forces. The monolithic structure with the plug-and-play design makes the SoftER easy to mount in less than one minute. Finally, due to the hyperelastic materials used for its construction the SoftER is washable and can resist to chemicals and a wide range of temperatures. Currently, the SoftER actuator in the prototype level consists of three main components (pneumatic fitting, housing, SPA) and costs approximately 10€ given the retail cost of pneumatic fitting and raw material volume. Both assembly sub-components and actuator cost are significantly smaller than current solutions, with cost even being an order of magnitude smaller.

In the future, further work is planned to improve the performance through testing a range of different silicone materials dedicated to the selected application. For the industrial scalability of the actuator we also plan to consider industrial grade elastomers, and vulcanised rubbers through industrial manufacturing processes such as injection molding with integrated components for pre-programming movement (e.g. pre-placed rings, celluloid strip inextensible layer). This will enable us to move from a labor-intensive prototyping fabrication process to an efficient industrial manufacturing scheme. Additionally, we intend to experiment with higher order parameters that fall beyond the solution space presented in this work. Moreover, we aim to further develop our concept from a module-focused level to a scaled system level. Towards that goal we plan on further developing our work to be validated as part of a higher-level architecture where we will further study and design the interfaces with other subsystems such as the imaging subsystem to detect faulty objects, pneumatic power supply circuit and unit design, software architecture, and dedicated soft controller design. To validate the industrial adaptation of the proposed actuator, we plan to perform two studies in follow-up work: (i) A benchmarking study to test and validate the robustness of the proposed actuator. Such study would include tests that pertain to the longevity and reliability of our design. These tests would include cycle loading testing, downtime analysis based on maintenance and installation times, and dedicated controller design and integration; (ii) A comparative analysis to place our system in the sorting machine landscape in terms of cost, performance, and ease of use. Such systems could be publicly available and potentially pursuing a collaboration with an industrial partner, so a comparative piloting experiment with current practices to calculate appropriate Key Performance Indicators (KPIs), can be conducted. Other examples to increase the operational robustness of the actuator would be to test vacuum retraction methods to decrease the rejection cycle, benchmark against current industrial solutions, and test actuator arrays instead of single modules. To further increase the robustness of the proposed work we intend to investigate in more detail the experimental results in contrast with the simulated ones by additionally using more computationally driven optimisation methods such as Genetic Algorithm (GA) optimization that would require an integrated algorithmic approach through ABAQUS python scripting for both actuator design and modeling. Finally, experiments with different size and weight objects (>150 g), as well as higher speeds (>1 m/s), will be performed in a pilot study to assess the actuator's scalability and capacity to operate in realistic settings.

REFERENCES

[1] Grand View Research, "Global sorting machines market size, share & trends analysis report by end use (mining, food & beverage, pharmaceutical), product (weight sorter, optical sorter), region (eu, apac), and segment forecasts," pp. 2021–2028, Rep. GVR-4-68039-673-5, 2021.

[2] H.-R. Manouchehri, "Sorting: Possibilitis, limitations and future," in *Proc. Conf. Minerals Eng.*, 2003, pp. 2–16.

[3] G. Hamid, B. Deefholts, N. Reynolds, D. McCambridge, K. Mason-Palmer, and C. Briggs, "Automation and robotics for bulk sorting in the food industry," in *Robotics and Automation in the Food Industry*. Amsterdam, The Netherlands: Elsevier, 2013, pp. 267–287.

[4] I. Baek, B. K. Cho, and Y. S. Kim, "Development of a compact quality sorting machine for cherry tomatoes based on real-time color image processing," in *Proc. 4th Int. Workshop Comput. Image Anal. Agriculture*, 2012, pp. 1–6.

[5] O. O. Arjenaki, P. A. Moghaddam, and A. M. Motlagh, "Online tomato sorting based on shape, maturity, size, and surface defects using machine vision," *Turkish J. Agriculture Forestry*, vol. 37, pp. 62–68, 2013.

[6] A. Istiadi, S. R. Sulistiyanti, Herlinawati, and H. Fitriawan, *Model Design of Tomato Sorting Machine Based on Artificial Neural Network Method using Node MCU Version 1.0*, vol. 1376. Bristol, U.K: Inst. Phys. Publishing, Nov. 2019.

[7] J. Thompson et al., "Harvest mechanization helps agriculture remain competitive," *California Agriculture*, vol. 54, no. 3, pp. 51–56, 2000.

[8] B. Mosadegh et al., "Pneumatic networks for soft robotics that actuate rapidly," *Adv. Funct. Mater.*, vol. 24, no. 15, pp. 2163–2170, 2014.

[9] M. T. Tolley et al., "An untethered jumping soft robot," in *Proc. IEEE/RSJ Int. Conf. Intell. Robots Syst.*, 2014, pp. 561–566.

[10] Z. Zhang, X. Wang, D. Meng, and B. Liang, "Bioinspired spiral soft pneumatic actuator and its characterization," *J. Bionic Eng.*, vol. 18, no. 5, pp. 1101–1116, 2021.

[11] E. Perez-Guagnelli and D. D. Damian, "Deflected versus preshaped soft pneumatic actuators: A design and performance analysis toward reliable soft robots," *Soft Robot.*, vol. 9, no. 4, pp. 713–722, 2022.

[12] J. Walker et al., "Soft robotics: A review of recent developments of pneumatic soft actuators," in *Actuators*, vol. 9, 2020, Art. no. 3.

[13] P. Polygerinos et al., "Soft robotics: Review of fluid-driven intrinsically soft devices; manufacturing, sensing, control, and applications in human-robot interaction," *Adv. Eng. Mater.*, vol. 19, no. 12, 2017, Art. no. 1700016.

[14] M. Manti, V. Cacucciolo, and M. Cianchetti, "Stiffening in soft robotics: A review of the state of the art," *IEEE Robot. Automat. Mag.*, vol. 23, no. 3, pp. 93–106, Sep. 2016.

[15] C. Laschi, B. Mazzolai, and M. Cianchetti, "Soft robotics: Technologies and systems pushing the boundaries of robot abilities," *Sci. Robot.*, vol. 1, no. 1, 2016, Art. no. eaah3690.

[16] D. Rus and M. T. Tolley, "Design, fabrication and control of soft robots," *Nature*, vol. 521, no. 7553, pp. 467–475, 2015.

[17] T. Cook, "Spirals in nature and art," *Nature*, vol. 68, no. 1761, p. 296, 1903.

[18] S. Guo, L. Yang, Y. Yuan, Z. Zhang, and X. Cao, "Elastic energy storage technology using spiral spring devices and its applications: A review," *Energy Built Environ.*, vol. 4, no. 6, pp. 669–679, 2022.

[19] J. Holt, "Design and testing of a biomimetic pneumatic actuated seahorse tail inspired robot," 2017. [Online]. Available: https://tigerprints.clemson.edu/all_theses/2637

[20] Z. Lu, E. Cao, K. Wang, T. Mei, X. Wu, and Q. Zhang, "A catapult robot with chameleon-inspired multi-body elastic nested system," in *Proc. IEEE Int. Conf. Robot. Biomimetics*, 2017, pp. 706–711.

[21] V. Ramses et al., "Robotic tentacles with three–dimensional mobility based on flexible elastomers," *Adv. Mater.*, vol. 25, no. 2, pp. 205–212, 2013.

[22] W. Fonseca, J. Ristow, D. Sanches, and S. Gerges, "A different approach to archimedean spiral equation in the development of a high frequency array," vol. 10, 2010.

[23] G. Anatriello and G. Vincenzi, "Logarithmic spirals and continue triangles," *J. Comput. Appl. Math.*, vol. 296, pp. 127–137, 2016. [Online]. Available: https://doi.org/10.1016/j.cam.2015.09.004

[24] L. Marechal, P. Balland, L. Lindenroth, F. Petrou, C. Kontovounisios, and F. Bello, "Toward a common framework and database of materials for soft robotics," *Soft Robot.*, vol. 8, no. 3, pp. 284–297, 2021.

[25] P. Polygerinos et al., "Modeling of soft fiber-reinforced bending actuators," *IEEE Trans. Robot.*, vol. 31, no. 3, pp. 778–789, Jun. 2015.